Dependance of isoprene emission flux on leaf mass per area of Phyllostachys pubescens (moso bamboo)

AUTHOR(S):

CHANG, Ting-Wei; KOSUGI, Yoshiko; KUME, Tomonori; KATAYAMA, Ayumi; OKUMURA, Motonori; CHANG, Ken-Hui

CITATION:

CHANG, Ting-Wei ...[et al]. Dependance of isoprene emission flux on leaf mass per area of Phyllostachys pubescens (moso bamboo). Journal of Agricultural Meteorology 2022, 78(1): 1-7

ISSUE DATE:

2022

URL:

http://hdl.handle.net/2433/278957

Open Access
Full Paper

Journal of Agricultural Meteorology 78(1): 1–7, 2022

Dependance of isoprene emission flux on leaf mass per area of *Phyllostachys pubescens* (moso bamboo)

Ting-Wei CHANG[a,†], Yoshiko KOSUGI[a], Tomonori KUME[c], Ayumi KATAYAMA[c], Motonori OKUMURA[b] and Ken-Hui CHANG[d]

[a] Graduate School of Agriculture, Kyoto University, Kyoto 606–8502, Japan
[b] Research Institute of Environment, Agriculture and Fisheries, Osaka Prefecture, Habikino, Osaka 583–0862, Japan
[c] Shiiba Research Forest, Kyushu University, Miyazaki 883–0402, Japan
[d] Department of Safety, Health and Environmental Engineering, National Yunlin University of Science and Technology, Yunlin 64002 Taiwan

Abstract

It is challenging to estimate isoprene emissions from plants and determine the basal isoprene emission rate (i.e., isoprene emission capacity under a specific light and leaf temperature) of plant species. Previous studies have investigated the effect of physiological factors on isoprene emission capacity; however, the effect of leaf morphology on isoprene emission capacity has seldom been mentioned. This study aims to clarify the relationship between the basal isoprene emission rate and leaf mass per area (LMA) of a woody bamboo (*Phyllostachys pubescens*). Since there was no observation of isoprene emission from low-LMA leaves of *P. pubescens*, we conducted measurements on culms exhibiting lower LMA (27.5–47.9 g m^{-2}). By observing leaf-scale isoprene emission flux under a specific incident light (1000 μmol m^{-2} s^{-1}) and temperature (30 ℃) to represent basal isoprene emission fluxes, we found a series of varied area-based isoprene emission rate among leaves (1.4–32.2 nmol m^{-2} s^{-1}) and a strong correlation between area-based isoprene emission rate and LMA without any distinction between culms. A further comparison with other studies demonstrated that even for the culms that exhibited larger LMA and isoprene emission flux, a generally consistent pattern in the relation of area-isoprene emission flux and LMA could be found across these sites. This result suggests the importance of detecting LMA in the determination of the basal isoprene emission rate, which can improve the current emission estimation method.

Key words: *Bambusoideae*, Basal isoprene emission rate, Biogenic volatile organic compound, Emission inventory

1. Introduction

Largescale emissions of isoprene from vegetation have been revealed by several global estimation studies, which show that plant-based emissions can be 4–7 times the global anthropogenic emissions of non-methane volatile organic compound emissions (Guenther *et al*., 2006; Guenther *et al*., 2012; Kansal, 2009; Saunois *et al*., 2020; Sindelarova *et al*., 2014). The emission of isoprene can affect atmospheric chemistry and cause negative effects such as the formation of air pollution (e.g., ozone, oxidants, and secondary organic aerosols) with nitrogen oxides (Claeys *et al*., 2004; Kanakidou *et al*., 2005; Paulson and Seinfeld, 1992; Teng *et al*., 2017); moreover, isoprene emissions can alter the global warming potential by changing the lifetime of methane and as a carbon emission itself (Archibald *et al*., 2011; Fehsenfeld *et al*., 1992; Pike and Young 2009). The assessment of global isoprene emissions is necessary for the mitigation of isoprene-induced negative effects.

Received; May 18, 2021
Accepted; August 30, 2021
†Corresponding author: tingwei.chang.85c@st.kyoto-u.ac.jp
DOI: 10.2480/agrmet.D-21-00030

The current global estimation of isoprene emissions, such as the Model of Emissions of Gases and Aerosols from Nature (MEGAN, Guenther *et al*., 2006) combines meteorological data, land use maps, emission inventories (i.e. basal isoprene emission, the isoprene emission capacity under a specific light and leaf temperature), activity factors including responses to light, temperature, leaf age, soil moisture, leaf area index, and CO_2 inhibition. It has been shown that estimation results are highly sensitive to emission inventory (Henrot *et al*., 2017). Since isoprene emission capacity could change among different species and have intraspecific variation, determination of emission inventory should be carefully obtained from field observations or scientific estimations.

Recent reports have indicated that, *Phyllostachys pubescens* (moso bamboo), a woody bamboo that exhibits invasion and expansion (Akutsu *et al*., 2012; Bai *et al*., 2013; Kudo *et al*., 2011; Takada *et al*., 2012), showed a potential of high isoprene emission, however, with discrepancies in basal isoprene emission flux detected among sites, or even among leaves. (Chang *et al*., 2019; Okumura *et al*., 2018).

Physiology-linked factors (e.g., temperature, leaf nitrogen concentration, photosynthetic limitations) of isoprene emission capacity of the plant leaves have been well shown by previous studies (e.g., Beckett *et al*., 2012; Litvak *et al*., 1996; Niinemets *et al*., 1999; Oku *et al*., 2014; Rosenstiel *et al*., 2004). Currently, however, knowledge of the relationship between morphologic

effect and isoprene emission is limited, only Harley *et al*. (1997) reported that sunlit leaves with higher leaf mass per area (LMA) showed higher area-based isoprene emission rate than shaded leaves for deciduous oak species. Because leaf morphology could determine the abundance of chloroplast in unit area, the area-based isoprene emission flux is expected to respond to the change in leaf morphology since the production of isoprene is dependent to chloroplast. Therefore, by clarifying the relationship between leaf morphology and isoprene emission, a better determination of the emission factor for isoprene could be achieved.

According to previous research, LMA could be an indicator of number of chloroplasts per area (Hanba *et al*., 1999; Ivanova *et al*., 2018; Liakoura *et al*., 2009), therefore, this study hypothesizes a linkage between area-based isoprene emission flux and LMA to explain the variation in isoprene emission capacity for moso bamboo and aims to determine the relationship between isoprene emission capacity and LMA. To test this hypothesis, we conducted isoprene emission measurements in constant environmental conditions on a hillslope that demonstrates a high morphological diversity for moso bamboo culms. It has been showed that the LMA of moso bamboo leaves could vary largely, from 25 to 70 g m^{-2} (Lin *et al*., 2020), but only isoprene emission from leaves with higher LMA (> 55 g m^{-2}) has been observed (e.g., Chang *et al*., 2019; Chang *et al*., under submission). Due to the lack of isoprene emission observations of moso bamboo leaves with LMA of < 55 g m^{-2}, this study conducted measurements on leaves of overtopped moso bamboo culms to fill the gap in isoprene emission traits with lower LMA. Because the photosynthetic rate and nitrogen concentration could also influence isoprene emission capacity (Harley *et al*., 1994; Litvak *et al*., 1996; Niinemets *et al*., 1999; Rasulov *et al*., 2009; Rosenstiel *et al*., 2004), we also recorded these factors to help in determining the attribution of LMA.

2. Materials and methods

2.1. Site description

The field work was conducted in an unmanaged pure moso bamboo stand on a hillslope in Fukuoka Prefecture, Japan (33°38' N, 130°33' E) with a slope angle of 42.8°. This site has a subtropical monsoon climate with an average annual temperature of 15.9 ℃ and annual precipitation of 1833 mm. Average culm density, diameter at breast height (DBH), and height of 8000 ± 480 culms per hectare, 9.5 ± 0.7 cm, and 11.1 ± 0.7 m were recorded, respectively. Previous investigations of vegetation and soil indicated large spatial variations in culm density, culm height, DBH, biomass distribution, soil nitrogen content, and soil moisture at this site (Ichihashi *et al*., 2015; Shimono *et al*., 2021). Eight moso bamboo culms (Culm A to Culm H) were chosen for measurement at the site, each of which demonstrated different DBH and culm height; the age of these culms were less than two years during measurement. Note that the chosen culms demonstrated lower culm height (4.2–7.9 m) and DBH (2.0–5.2 cm) to their neighboring culms and had weaker light exposure than the top of the canopy (Table 1). For each culm, four leaves near the top of the crown were measured for isoprene emission flux, photosynthetic rate, nitrogen concentration, and LMA.

2.2. Measurements

In this study, the culm height and DBH for each of the selected culms were measured, as were the isoprene emission flux, photosynthetic rate, LMA, and nitrogen concentration for each of the chosen leaves.

The measurement period of isoprene emission rate and photosynthetic rate was August 14–17, 2019. A portable photosynthesis measuring system (LI-6400, Li-Cor Inc., Lincoln, NE, USA) equipped with an LED cuvette (LI-6400-02B, Li-Cor Inc.) was used to conduct the measurements. To capture isoprene, a T-junction (made of Teflon to avoid adsorption of VOCs) was added to replace the original tube between the leaf cuvette of LI-6400 and its embedded infrared gas analyzer (IRGA), adding another channel that can be plugged to an adsorbent tube; a granular filter filled with activated charcoal was connected to the air inlet of the LI-6400 system to supply VOC-free air. The adsorbent tube used for isoprene collection is made of glass and filled with 250 mg Tenax-TA 60/80 mesh (GL Science Inc., Tokyo, Japan), based on the method tested and verified by Chang (2009).

During sampling, the light and leaf temperatures in the cuvette were set at a photosynthetic photon density flux (PPFD) of 1000 μmol m^{-2} s^{-1} and a temperature of 30 ℃. Leaves were clamped by the leaf cuvette for approximately 5 min to stabilize gas exchange under the controlled light and leaf temperatures. During this period, the photosynthetic rate was recorded once it

Table 1. DBH, culm height, leaf mass per area (LMA), area-based isoprene emission flux (I_{Area}), mass-based isoprene emission flux (I_{Mass}), area-based photosynthetic rate (A_{Area}), mass-based photosynthetic rate (A_{Mass}), area-based leaf nitrogen concentration (N_{Area}), and mass-based leaf nitrogen concentration (N_{Mass}) of each moso bamboo culm. (Mean ± standard deviation)

Culm	I_{Area} (nmol m^{-2} s^{-1})	I_{Mass} (μg g^{-1} hr^{-1})	LMA (g m^{-2})	A_{Area} (μmol m^{-2} s^{-1})	A_{Mass} (mg g^{-1} hr^{-1})	N_{Area} (g m^{-2})	N_{Mass} (%)	DBH (cm)	Height (m)
A	24.1 ± 6.0	135.4 ± 28.8	43.6 ± 4.6	4.8 ± 2.1	17.3 ± 6.9	1.2 ± 0.2	2.7 ± 0.2	2.7	5.9
B	16.4 ± 6.2	104.3 ± 42.6	39.5 ± 5.0	5.3 ± 2.7	22.0 ± 11.6	1.0 ± 0.1	2.5 ± 0.1	3.9	6.8
C	14.5 ± 3.8	95.3 ± 24.8	37.3 ± 1.3	4.7 ± 1.4	20.0 ± 5.6	1.0 ± 0.1	2.6 ± 0.1	5.0	7.9
D	11.7 ± 5.2	90.6 ± 45.3	32.4 ± 2.6	3.9 ± 2.2	18.6 ± 10.2	0.8 ± 0.1	2.6 ± 0.2	2.0	4.7
E	11.4 ± 3.0	87.1 ± 18.1	31.8 ± 2.3	2.2 ± 1.2	11.2 ± 5.8	0.9 ± 0.1	2.8 ± 0.1	3.0	4.2
F	10.1 ± 2.3	83.9 ± 18.5	32.2 ± 1.0	3.3 ± 1.2	15.9 ± 5.7	0.9 ± 0.1	2.8 ± 0.3	3.3	6.9
G	8.6 ± 7.5	59.2 ± 48.3	34.7 ± 2.7	4.6 ± 1.6	20.9 ± 6.4	0.9 ± 0.1	2.5 ± 0.2	5.2	7.9
H	5.3 ± 5.0	43.6 ± 40.3	29.2 ± 1.2	2.2 ± 1.4	11.6 ± 7.6	0.9 ± 0.0	3.1 ± 0.0	2.6	6.7

became steady; after this period, an adsorbent tube was plugged into the T-junction channel on one side and a micropump (MP-Σ30NII, SIBATA Inc., Tokyo, Japan) on the other side. The pumping rate was set at 150 mL min^{-1} to draw out the air from the leaf cuvette for 400 s. Air (1 L) was passed through the adsorbent tube to trap the isoprene component. The collected adsorbents were stored at a temperature of approximately 5 ℃ for less than 14 days until isoprene levels were quantified. The area-based photosynthetic rate (A_{Area}, μmol m^{-2} s^{-1}) and mass-based photosynthetic rate (A_{Mass}, mg g^{-1} hr^{-1}) were determined as follows:

$$A_{Area} = A_{Origin} \cdot R_{Cuvette}/R_{Origin} \quad (1)$$

$$A_{Mass} = A_{Area} \cdot M_{CO_2} \cdot R_{Leaf}/M_{Leaf} \quad (2)$$

where A_{Origin} (μmol m^{-2} s^{-1}) is the measured value of the photosynthetic rate with the default leaf area (R_{Origin}) set at 6 cm^2, $R_{Cuvette}$ (cm^2) is the actual in-cuvette leaf area, M_{CO_2} is the molecular mass of CO_2 (44.01 g mol^{-1}), R_{Leaf} (cm^2) and M_{Leaf} (g) are the whole leaf area and dry mass of the measured leaf, respectively.

The LMA (g m^{-2}) of the leaves was determined using R_{Leaf} and M_{Leaf}. To obtain R_{Leaf}, the leaves were scanned rapidly after excision with a scanner (GT-S650, Seiko Epson Corporation, Nagano, Japan) before deformation due to dehydration, and measured using an image processing software (ImageJ, National Institutes of Health, Bethesda, MD, USA). The scanned leaves were then dried in an oven at 60 ℃ for 72 h for M_{Leaf} measurement with a microbalance (accuracy: 0.1 mg).

The quantification of isoprene emissions was determined by gas chromatography-mass spectrometry. The isoprene content in the adsorbent tube was first desorbed and re-trapped with a preconcentrator (Model 7100A, Entech Instruments Inc., CA, USA), and then introduced into a gas chromatography system with a mass spectrometer (HP6890, Agilent Technologies Inc., CA, USA) for identification and quantification. A calibration line ($R^2 > 0.995$) was obtained by testing standard samples at different isoprene concentrations (5, 10, 20, 50, and 100 ppb) with the same air flow as the actual field measurements. The obtained isoprene concentration ($C_{Isoprene}$) was then used to calculate the area-based isoprene emission flux (I_{Area}, nmol m^{-2} s^{-1}) and mass-based isoprene emission flux (I_{Mass}, μg g^{-1} hr^{-1}) using the following equation:

$$I_{Area} = C_{Isoprene} \cdot F/R_{Cuvette} \quad (3)$$

$$I_{Mass} = I_{Area} \cdot M_{isoprene} \cdot R_{Leaf}/M_{Leaf} \quad (4)$$

where F (μmol s^{-1}) is the flow rate of the LI-6400 air inflow, and $M_{isoprene}$ is the molecular mass of isoprene (68.12 g mol^{-1}).

The whole leaf nitrogen content ($N_{Content}$, mg) was determined using an element analyzer (JM1000 system, J-SCIENCE LAB, Co., Ltd., Japan) based on the Pregl-Dumas method. A calibration line ($R^2 > 0.999$) was established by testing the standard material (hippuric acid, $C_9H_9NO_3$) in different masses (3, 6, 9, 20, 30, and 50 mg). Area-based nitrogen concentration (N_{Area}, g m^{-2}) and mass-based nitrogen concentration (N_{Mass}, %) are defined as follows:

$$N_{Area} = N_{Content}/R_{Leaf} \quad (5)$$

$$N_{Mass} = N_{Content}/M_{Leaf} \quad (6)$$

3. Results

The moso bamboo culms selected for measurement exhibited various morphologies, with differing DBH and culm height measured; observations including I_{Area}, I_{Mass}, LMA, A_{Area}, A_{Mass}, N_{Area}, and N_{Mass} also demonstrated variations among culms (Table 1). Even under the same irradiance (PPFD = 1000 μmol m^{-2} s^{-1}) and leaf temperature (~30 ℃), large variations in isoprene emission fluxes were recorded

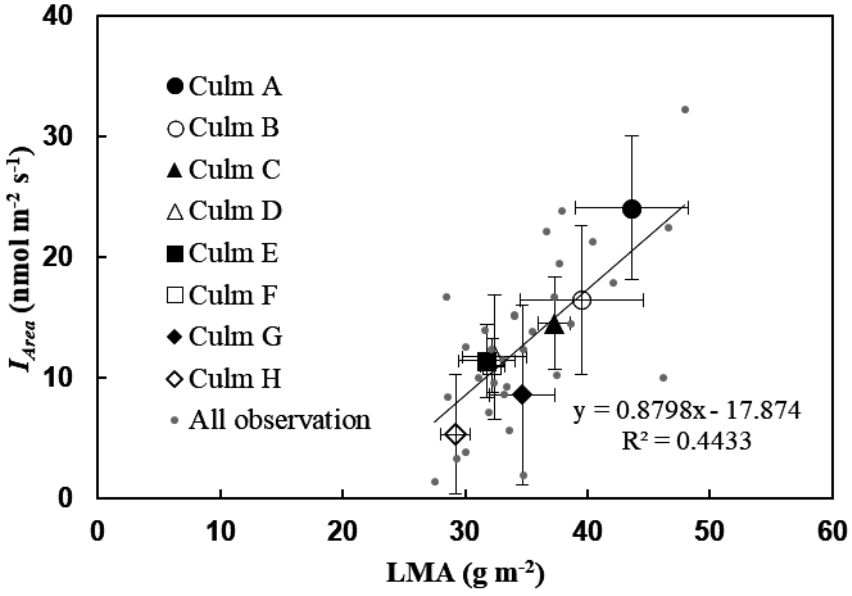

Fig. 1. Relationship between leaf mass per area (LMA) and area-based isoprene emission flux (I_{Area}). Gray dots represent all the observations. Solid and open circle, triangle, square, and diamond represent observation averages with standard deviation error bars (N = 4) from different culm.

(I_{Area}: 1.4–32.2 nmol m^{-2} s^{-1}; I_{Mass}: 12.4–164.8 μg g^{-1} hr^{-1}). The observed factors also demonstrated variations among leaves, where LMA exhibited a range of 27.5–47.9; A_{Area} and A_{Mass} exhibited ranges of 0.6–7.7 μmol m^{-2} s^{-1} and 3.5–31.4 mg g^{-1} hr^{-1}, respectively; N_{Area} and N_{Mass} exhibited ranges of 0.7–1.4 g m^{-2} and 2.3–3.3 %.

I_{Area} and I_{Mass} were more likely to be associated with varying leaf morphology instead with DBH or culm height though the culms exhibited a large variety in these culm morphologies (Table 1). As shown in Fig. 1, I_{Area} significantly increased with LMA. Basing on Pearson' r value (R) and t-test P value (P), a strong correlation between I_{Area} and LMA ($P < 0.001$; $R = 0.666$) were observed, and LMA was determined to be the most significant factor influencing I_{Area}; the effect of LMA on I_{Mass} was less, but still significant (Table 2).

Both A_{Area} and N_{Area} exhibited significant positive correlations with I_{Area} (Table 2). No relationship was detected, however, between N_{Mass} and I_{Mass} or between A_{Mass} and I_{Mass}. Note that all three observations in the area-based units demonstrated strong correlations with LMA, which explained most of the variation in them (Table 2).

By comparing our results with other studies on isoprene emission from moso bamboo (Chang *et al*., 2019; Chang *et al*., under submission), we can see that I_{Area} in this study was remarkably lower than those in other studies (Fig. 2a). These three sites had different stand characteristics. The site of Chang *et al*. (2019) was in a pure moso bamboo stand in central Taiwan under an influence of humid subtropical climates. This site grows well-grown culms with a height of 15 m, and the measured leaf demonstrated the largest LMA among the sites (77.7 ± 16.3 g m^{-2}). The data selected for comparison of this site were recorded in September 2015 with a leaf temperature of 25.7 ± 1.6 ℃ and PPFD of 1000 μmol m^{-2} s^{-1}. The site of Chang *et al*. (under submission) was in a specimen garden in Kyoto, Japan. Although the height of the measured culm was relatively low (6.5 m), the leaves were well exposed to sunlight due to a far distribution between each culm at this site and demonstrated a moderate LMA among the sites (52.7 ± 2.3 g m^{-2}). The data collected from this site were recorded in August 2019 with a leaf temperature of 31.4 ± 1.0 ℃ and a PPFD of 1000 μmol m^{-2} s^{-1}.

Table 2. Pearson correlation coefficient and significance of correlation determined by t-test p-value of each pair between area-based isoprene emission flux (I_{Area}), mass-based isoprene emission flux (I_{Mass}), leaf mass per area (LMA), area-based photosynthetic rate (A_{Area}), mass-based photosynthetic rate (A_{Mass}), area-based leaf nitrogen concentration (N_{Area}), and mass-based nitrogen concentration (N_{Mass}).

	I_{Area}	I_{Mass}	LMA	A_{Area}	A_{Mass}	N_{Area}	N_{Mass}
I_{Area}	---						
I_{Mass}	.950***	---					
LMA	.666***	.437*	---				
A_{Area}	.432*	.315	.507***	---			
A_{Mass}	.255	.190	.292	.964***	---		
N_{Area}	.586***	.352	.816***	.325	.115	---	
N_{Mass}	–.227	–.227	–.364*	–.363	–.340	.235	---

*p-value < .05; **p-value < .01; ***p-value < .001

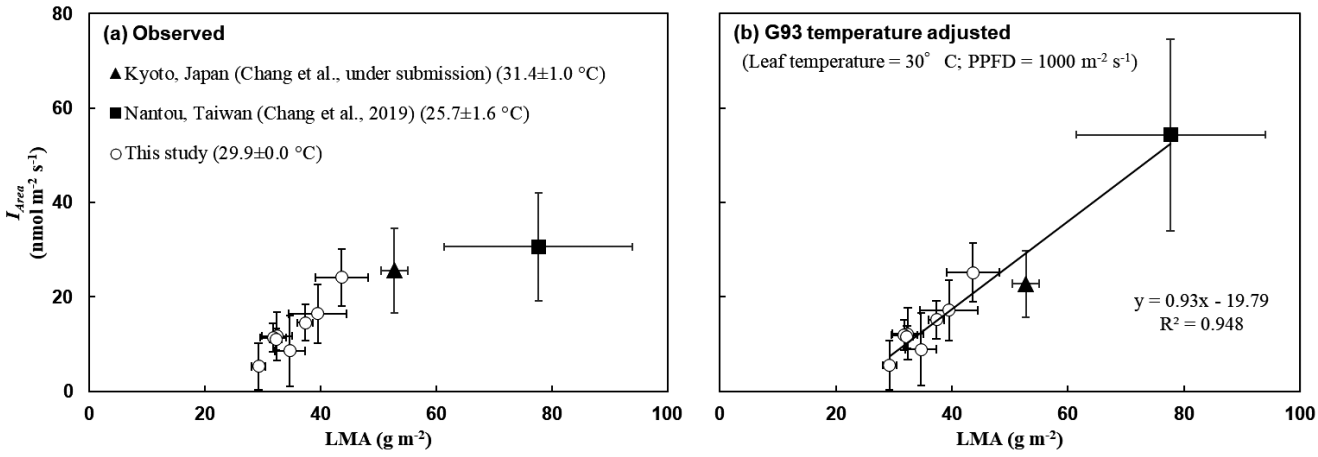

Fig. 2. Relationship between (a) leaf mass per area (LMA) and area-based isoprene emission flux (I_{Area}), and (b) LMA and I_{Area} adjusted by G93 algorithm (Guenther *et al*., 1993) in different sites (This study, Chang *et al*., 2019, and Chang *et al*., under submission). Open circles represent the observation averaged by each culm in this study (N = 4 per culm, leaf temperature = 29.9 ± 0.0 ℃); solid square represents the averaged observation from a newly abandoned moso bamboo stand in Taiwan conducted by Chang *et al*., 2019 (N = 4, leaf temperature = 25.7 ± 1.6 ℃); solid triangle represents the averaged observation from a moso bamboo plot in a specimen garden in Kyoto conducted by Chang *et al*., under submission (N = 3; leaf temperature = 31.4 ± 1.0 ℃).

With I_{Area} adjusted by the G93 model (Guenther *et al*., 1993) to simulate a temperature of 30 ℃ and PPFD of 1000 μmol m^{-2} s^{-1}, a pattern between the adjusted I_{Area} and LMA that was generally consistent across the different sites is demonstrated (Fig. 2).

4. Discussion

According to Poorter *et al*. (2009), leaf morphology is strongly related to light of growth environment in most vegetation. Furthermore, bamboo leaves grown under shaded condition were reported to be thinner than leaves grown under sunlit condition (March and Clark, 2011). Therefore, a lower LMA would be expected in the overtopped moso bamboo culms in this site. These overtopped leaves demonstrated lower LMA (27.5–47.9 g m^{-2}) when compared to recorded averages according to Lin *et al*. (2020). The large range of LMA recorded in this study could be due to the consequently various canopy gap sizes to the large spatial variation in culm density in this site. Even under the same incident light and temperature, isoprene emission fluxes demonstrated large variance among the leaves in this study. By plotting the isoprene emission fluxes and LMA, we found that LMA explained most of the variation in I_{Area} and part of the variation in I_{Mass}. Considering the measurements in a previous study on moso bamboos (i.e., Chang *et al*., 2019; under submission) conducted under similar incident light and season, a consistent pattern was observed between the I_{Area} and LMA across these sites. The linkage between I_{Area} and LMA could be explained by the higher quantity of chloroplasts per unit leaf area for leaves with higher LMA. According to an allometry study of bamboo species, leaf density is proportional to about -3/4 power of leaf thickness (Lin *et al*., 2018). Since LMA can be decomposed as the product of leaf density and leaf thickness (LMA = leaf density × leaf thickness), a higher LMA implies thicker mesophylls, which tend to have larger chloroplasts per area (Hanba *et al*., 1999; Ivanova *et al*., 2018; Liakoura *et al*., 2009); isoprene is produced only by chloroplasts in leaves (Sasaki *et al*., 2005; Wildermuth and Fall, 1996; Wildermuth and Fall, 1998), meaning a larger quantity of chloroplasts per area could induce larger I_{Area} at the leaf scale. Nevertheless, the amount of chloroplast per area or efficiency of chloroplast could be affected by many factors confound with LMA (e.g., water stress, growth temperature, and growth light) (Gamble and Burke, 1984; Gotoh *et al*., 2018; Taylor and Craig, 1971). Thus, further research is needed to identify actual mechanism causing the dependence on LMA of I_{Area}.

The positive correlation between I_{Mass} and LMA (Table 2) could be partially explained by an increased proportion of mesophyll in leaves with larger LMA. The linkage between these factors also infers potential effects from factors beyond morphological characteristics, indicating that leaves with higher LMA may exhibit more efficient isoprene production per unit mass. By analyzing the effect from nitrogen concentration and photosynthetic rate on isoprene emission capacity, we detected correlations between I_{Area}, N_{Area}, and A_{Area} (Table 2). However, since I_{Area}, N_{Area}, and A_{Area} were all demonstrated strong correlations with LMA, LMA could be a confounding variable and lead to spurious correlations between N_{Area} and I_{Area} and between A_{Area} and I_{Area}. To exclude this effect, we analyzed the mass-based form and found no correlation between A_{Mass} and I_{Mass}, nor between N_{Mass} and I_{Mass}. Since nitrogen in ammonium form could potentially enhance isoprene production by enlarging the substrate (dimethylallyl diphosphate) pool of isoprene synthesis (Rosenstiel *et al*., 2004), no correlation between I_{Mass} and N_{Mass} implies that the substrate for isoprene production was not constrained by nitrogen status of leaf during our measurement. The dependency of isoprene production on photosynthesis mainly comes from the energetic and reductive agents produced in light-dependent reactions. Previous studies have revealed that this dependency is more likely to relate to the electron transport chain rather than the whole photosynthesis process since photosynthetic rate could be limited by other factors such as stomatal conductance (Rodrigues *et al*., 2020). Although A_{Mass} did not explain I_{Mass}, we could not exclude the effect of electron transport rate, which has been reported to have a significant influence on isoprene emissions (Rasulov *et al*., 2009).

5. Conclusion

This study measured isoprene emission flux from low-LMA moso bamboo leaves under a constant light of 1000 μmol m^{-2} s^{-1} and leaf temperature of ~30 ℃. By combining the observations of moso bamboo with higher LMA conducted in previous studies, we verified a consistency between isoprene emission capacity and LMA of moso bamboo leaf under a variety of LMA. Because area-based isoprene emission capacity is a critical factor in current global-scale isoprene emission estimation methods, the detection of LMA can provide a better way to determine the isoprene emission capacity of plant leaves.

Acknowledgement

This work is supported by The Coca-Cola Foundation and JSPS KAKENHI (21K12275; 19H02996). We would like to express appreciation to Kyushu University Forest for providing site and bamboo material. We would also like to express appreciation to Dr. Yeou-Lih Yan (Professor of Department of Safety, Health and Environmental Engineering, National United University), and Mrs. Yi-Jen Pan (Research Assistant of Department of Safety, Health and Environmental Engineering, National Yunlin University of Science and Technology) to provide technical supports in VOCs analysis.

Reference

Akutsu H, Aizawa M, Matsue K *et al*., 2012: Distribution and invasion of *Phyllostachys pubescens* stands into neighboring forests in Nasukarasuyama, Tochigi Prefecture. *Bulletin of the Utsunomiya University Forests* **48**, 139–152.

Archibald AT, Levine JG, Abraham NL *et al*., 2011: Impacts of HOx regeneration and recycling in the oxidation of isoprene: Consequences for the composition of past, present and future atmospheres. *Geophysical Research Letters* **38**(5), [L05804]. https://doi.org/10.1029/2010GL046520

Bai S, Zhou G, Wang Y *et al*., 2013: Plant species diversity and dynamics in forests invaded by Moso bamboo (*Phyllostachys edulis*) in Tianmu Mountain Nature Reserve. *Biodiversity Science* **21**(3), 288–295. https://doi.org/10.3724/SP.J.1003.2013.08258

Beckett M, Loreto F, Velikova V *et al*., 2012: Photosynthetic limitations and volatile and non-volatile isoprenoids in the

poikilochlorophyllous resurrection plant *Xerophyta humilis* during dehydration and rehydration. *Plant, Cell & Environment* **35**(12), 2061–2074. https://doi.org/10.1111/j.1365-3040.2012.02536.x

Chang M, 2009: *Seasonal variations of C. Sinensis BVOCs flux measurements and its environmental factors at middle altitude in Taiwan* (Master's thesis, National Yunlin University of Science and Technology, Yunlin, Taiwan) Retrieved from https://hdl.handle.net/11296/cfx6en

Chang T, Kume T, Okumura M *et al*., 2019: Characteristics of isoprene emission from moso bamboo leaves in a forest in central Taiwan. *Atmospheric Environment* **211**, 288–295. https://doi.org/10.1016/j.atmosenv.2019.05.026

Claeys M, Graham B, Vas G *et al*., 2004: Formation of Secondary Organic Aerosols Through Photooxidation of Isoprene. *Science* **303**(5661) 1173–1176. https://doi.org/10.1126/science.1092805

Fehsenfeld F, Calvert J, Fall R *et al*., 1992: Emissions of volatile organic compounds from vegetation and the implications for atmospheric chemistry. *Global Biogeochemical Cycles* **6**(4), 389–430. https://doi.org/10.1029/92GB02125

Gamble PE, Burke JJ, 1984: Effect of water stress on the chloroplast antioxidant system: I. Alterations in glutathione reductase activity. *Plant physiology* **76**(3), 615–621. https://doi.org/10.1104/pp.76.3.615

Gotoh E, Suetsugu N, Higa T *et al*., 2018: Palisade cell shape affects the light-induced chloroplast movements and leaf photosynthesis. *Scientific Reports* **8**(1), 1472. https://doi.org/10.1038/s41598-018-19896-9

Guenther AB, Jiang X, Heald Colette L *et al*., 2012: The Model of Emissions of Gases and Aerosols from Nature Version 2.1 (MEGAN2.1): An Extended and Updated Framework for Modeling Biogenic Emissions. *Geoscientific Model Development* **5**(6), 1471–1492. https://doi.org/10.5194/gmd-5-1471-2012

Guenther A, Karl T, Harley P *et al*., 2006: Estimates of global terrestrial isoprene emissions using MEGAN (Model of Emissions of Gases and Aerosols from Nature). *Atmospheric Chemistry and Physics* **6**(11), 3181–3210. https://doi.org/10.5194/acp-6-3181-2006

Guenther AB, Zimmerman PR, Harley PC *et al*., 1993: Isoprene and monoterpene emission rate variability: model evaluations and sensitivity analyses. *Journal of Geophysical Research: Atmospheres* **98** (D7), 12609–12617.

Hanba YT, Miyazawa SI, Terashima I, 1999: The influence of leaf thickness on the CO_2 transfer conductance and leaf stable carbon isotope ratio for some evergreen tree species in Japanese warm-temperate forests. *Functional Ecology* **13**(5), 632–639. https://doi.org/10.1046/j.1365-2435.1999.00364.x

Harley P, Guenther A, Zimmerman P, 1997: Environmental controls over isoprene emission in deciduous oak canopies. *Tree Physiology* **17**(11), 705–714. https://doi.org/10.1093/treephys/17.11.705

Harley PC, Litvak ME, Sharkey TD *et al*., 1994: Isoprene Emission from Velvet Bean Leaves (Interactions among Nitrogen Availability, Growth Photon Flux Density, and Leaf Development). *Plant Physiology* **105**(1), 279–285. https://doi.org/10.1104/pp.105.1.279

Henrot AJ, Stanelle T, Schröder S *et al*., 2017: Implementation of the MEGAN (v2.1) biogenic emission model in the ECHAM6-HAMMOZ chemistry climate model. *Geoscientific Model Development* **10**(2), 903–926. https://doi.org/10.5194/gmd-10-903-2017

Ichihashi R, Komatsu H, Kume T *et al*., 2015: Stand-scale transpiration of two Moso bamboo stands with different culm densities. *Ecohydrology* **8**(3), 450–459. https://doi.org/10.1002/eco.1515

Ivanova LA, Yudina PK, Ronzhina DA *et al*., 2018: Quantitative mesophyll parameters rather than whole-leaf traits predict response of C3 steppe plants to aridity. *New Phytologist* **217**(2), 558–570. https://doi.org/10.1111/nph.14840

Kanakidou M, Seinfeld JH, Pandis SN *et al*., 2005: Organic aerosol and global climate modelling: a review. *Atmospheric Chemistry and Physics* **5**(4), 1053–1123. https://doi.org/10.5194/acp-5-1053-2005

Kansal A, 2009: Sources and reactivity of NMHCs and VOCs in the atmosphere: A review. *Journal of Hazardous Materials* **166**(1), 17–26. https://doi.org/10.1016/j.jhazmat.2008.11.048

Kudo G, Amagai Y, Hoshino B *et al*., 2011: Invasion of dwarf bamboo into alpine snow-meadows in northern Japan: pattern of expansion and impact on species diversity. *Ecology and Evolution* **1**, 85–96. https://doi.org/10.1002/ece3.9

Liakoura V, Fotelli MN, Rennenberg H *et al*., 2009: Should structure–function relations be considered separately for homobaric vs. heterobaric leaves?. *American Journal of Botany* **96**, 612–619. https://doi.org/10.3732/ajb.0800166

Lin S, Niklas KJ, Wan Y *et al*., 2020: Leaf shape influences the scaling of leaf dry mass vs. area: a test case using bamboos. *Annals of Forest Science* **77**(1), [11]. https://doi.org/10.1007/s13595-019-0911-2

Lin S, Shao L, Hui C *et al*., 2018: Why Does Not the Leaf Weight-Area Allometry of Bamboos Follow the 3/2-Power Law?. *Frontiers in Plant Science* **9**, 583. https://doi.org/10.3389/fpls.2018.00583

Litvak ME, Loreto F, Harley PC *et al*., 1996: The response of isoprene emission rate and photosynthetic rate to photon flux and nitrogen supply in aspen and white oak trees. *Plant, Cell & Environment* **19**(5), 549–559. https://doi.org/10.1111/j.1365-3040.1996.tb00388.x

March R and Clark L, 2011: Sun-shade variation in bamboo (Poaceae: Bambusoideae) leaves. *Telopea* **13**, 93–104. https://doi.org/10.7751/telopea20116007

Niinemets Ü, Tenhunen JD, Harley PC *et al*., 1999: A model of isoprene emission based on energetic requirements for isoprene synthesis and leaf photosynthetic properties for *Liquidambar* and *Quercus*. *Plant, Cell & Environment* **22**(11), 1319–1335. https://doi.org/10.1046/j.1365-3040.1999.00505.x

Oku H, Inafuku M, Takamine T *et al*., 2014: Temperature threshold of isoprene emission from tropical trees, *Ficus virgata* and *Ficus septica*. *Chemosphere* **95**, 268–273. https://doi.org/10.1016/j.chemosphere.2013.09.003

Okumura M, Kosugi Y, Tani A, 2018: Biogenic volatile organic compound emissions from bamboo species in Japan. *Journal of Agricultural Meteorology* **74**(1), 40–44. https://doi.org/10.2480/agrmet.D-17-00017

Paulson SE, Seinfeld JH, 1992: Development and evaluation of a photooxidation mechanism for isoprene. *Journal of Geophysical Research* **97**(D18), 20703–20715. https://doi.org/10.1029/92JD01914

Pike RC, Young PJ, 2009: How plants can influence tropospheric chemistry: the role of isoprene emissions from the biosphere. *Weather* **64**(12), 332–336. https://doi.org/10.1002/wea.416

Poorter H, Niinemets Ü, Poorter L *et al*., 2009: Causes and consequences of variation in leaf mass per area (LMA): a meta-analysis. *New Phytologist* **182**(3), 565–588. https://doi.org/10.1111/j.1469-8137.2009.02830.x

Rasulov B, Hüve K, Välbe M *et al*., 2009: Evidence that light, carbon dioxide, and oxygen dependencies of leaf isoprene emission

are driven by energy status in hybrid aspen. *Plant Physiology* **151**(1), 448–460. https://doi.org/10.1104/pp.109.141978

Rodrigues TB, Baker CR, Walker AP *et al*., 2020: Stimulation of isoprene emissions and electron transport rates as key mechanisms of thermal tolerance in the tropical species *Vismia guianensis*. *Global Change Biology* **26**(10), 5928–5941. https://doi.org/10.1111/gcb.15213

Rosenstiel TN, Ebbets AL, Khatri WC *et al*., 2004: Induction of Poplar Leaf Nitrate Reductase: A Test of Extrachloroplastic Control of Isoprene Emission Rate. *Plant Biology* **6**(1), 12–21. https://doi.org/10.1055/s-2003-44722

Sasaki K, Ohara K, Yazaki K, 2005: Gene expression and characterization of isoprene synthase from *Populus alba*. *FEBS Letters* **579**(11), 2514–2518. https://doi.org/10.1016/j.febslet.2005.03.066.

Saunois M, Stavert AR, Poulter B *et al*., 2020: The Global Methane Budget 2000–2017. *Earth System Science Data* **12**(3), 1561–1623. https://doi.org/10.5194/essd-12-1561-2020

Shimono K, Katayama A, Kume T *et al*., 2021: Differences in net primary production allocation and nitrogen use efficiency between Moso bamboo and Japanese cedar forests along a slope. *Journal of Forest Research*, published online. https://doi.org/10.1080/13416979.2021.1965280

Sindelarova K, Granier C, Bouarar I *et al*., 2014: Global data set of biogenic VOC emissions calculated by the MEGAN model over the last 30 years. *Atmospheric Chemistry and Physics* **14**(17), 9317–9341. https://doi.org/10.5194/acp-14-9317-2014

Takada M, Inoue T, Mishima Y *et al*., 2012: Geographical Assessment of Factors for Sasa Expansion in the Sarobetsu Mire, Japan. *Journal of Landscape Ecology* **5**(1), 58–71. https://doi.org/10.2478/v10285-012-0049-5

Taylor AO, Craig AS, 1971: Plants under Climatic Stress: II. Low Temperature, High Light Effects on Chloroplast Ultrastructure. *Plant Physiology* **47**(5), 719–725. https://doi.org/10.1104/pp.47.5.719

Teng AP, Crounse JD, Wennberg PO, 2017: Isoprene Peroxy Radical Dynamics. *Journal of the American Chemical Society* **139**(15), 5367–5377. https://doi.org/10.1021/jacs.6b12838

Wildermuth MC, Fall R, 1996: Light-Dependent Isoprene Emission (Characterization of a Thylakoid-Bound Isoprene Synthase in Salix discolor Chloroplasts). *Plant Physiology* **112**(1), 171–182. https://doi.org/10.1104/pp.112.1.171

Wildermuth MC, Fall R, 1998: Biochemical characterization of stromal and thylakoid-bound isoforms of isoprene synthase in willow leaves. *Plant Physiology* **116**(3), 1111–1123. https://doi.org/10.1104/pp.116.3.1111